Exchange Rates and Numbers of Annular Lipids for the Calcium and Magnesium Ion Dependent Adenosinetriphosphatase†

J. M. East,‡ D. Melville,§ and A. G. Lee*,‡

Departments of Biochemistry and Physics, University of Southampton, Southampton SO9 3TU, U.K.

Received March 20, 1984

ABSTRACT: A spin-labeled phospholipid is used to study lipid–protein interactions in the (Ca^{2+},Mg^{2+})-ATPase of sarcoplasmic reticulum from muscle. A novel null method is used to decompose composite electron spin resonance spectra into two components, characteristic of immobilized and mobile environments. Calculations based on a random mixing model suggest that protein–protein interactions will be relatively rare in these systems and that the immobilized lipid does not represent lipid trapped between proteins but rather represents annular phospholipid at the lipid–protein interface of the adenosinetriphosphatase. The apparent decrease in the amount of immobilized lipid with increasing temperature is shown to be consistent with lipid exchange between bulk and annulus, characterized by an exchange time of 10^{-7} s at 37 °C. A minimum number of annular phospholipid sites of 32 and 22 are calculated at 0 and 37 °C, respectively.

Biological membranes are complex heterogeneous mixtures of lipid and protein. An understanding of the structures adopted by such mixtures requires a knowledge of both lipid–lipid and lipid–protein interactions since this would allow calculation of the relative positions of all the components in the membrane. At present, it is only feasible to obtain such information for highly simplified membrane systems such as the (Ca^{2+},Mg^{2+})-ATPase purified from sarcoplasmic reticulum and reconstituted into phospholipid bilayers of defined phospholipid composition.

Although association of the (Ca^{2+},Mg^{2+})-ATPase with lipid bilayers is strong (as demonstrated by the difficulty in removing all the lipid from the ATPase system), there is little structural specificity in the interaction of phospholipids with the ATPase, since relative binding constants for a wide range of phospholipids in the liquid-crystalline phase are close to 1, although relative binding constants for phospholipids in the gel phase are low compared to those in the liquid-crystalline phase (London & Feigenson, 1981; East & Lee, 1982). This argues against the existence of discrete binding sites for phospholipids on the ATPase (comparable, for example, to the binding site for ATP), but rather for a hydrophobic surface on the ATPase with which the fatty acyl chains of the phospholipid can interact. Interaction with such a surface would be structurally undemanding so that on- and off-rate constants for phospholipids coming on and off the surface of the ATPase (entering and leaving the phospholipid annulus of the ATPase) would be expected to be comparable to the rate of diffusion of phospholipids in simple phospholipid bilayers. These rates can sometimes be estimated by using electron spin resonance (ESR).[1]

ESR spectra of spin-labeled phospholipids and fatty acids in a variety of lipid–protein systems show the coexistence of two spin-label populations whose exchange rate is slow on the ESR time scale ($\nu_{ex} \leq 10^8$ s^{-1}). Although there is still some controversy, one component is believed to correspond to spin-label in the bulk lipid bilayer component of the membrane whereas the other, immobilized component is thought to arise from spin-label in contact with membrane proteins [see Watts (1981)]. The annular lipid will be spatially disordered and exhibit reduced molecular motion because of its contact with the molecularly rough surface of the protein.

Unfortunately, methods for the decomposition of composite ESR spectra into the assumed two components are rather subjective. The most common method is to assume the line shape of one component and to subtract a given amount of that component from the composite to obtain the second component. The amount of the first component to be subtracted is chosen so that the line shape of the resulting second component is "reasonable". Such a procedure can be relatively inaccurate, particularly when the experimental spectra have a low signal-to-noise ratio (Jost & Griffith, 1978a; Griffith et al., 1982). If the first component is chosen to be the immobilized component, then it is often picked by matching the extreme splitting of the composite spectra to a set of spectra for immobilized spin-labels. Alternatively, the spectrum obtained at a very low molar ratio of lipid to protein for the system of interest can be assumed to be due solely to the immobilized component (Jost & Griffith, 1978b). If the first component is chosen to be the fluid component, then it can be chosen from a set of reference spectra for simple lipid bilayers at different temperatures (Watts et al., 1979). For some systems, an alternative method may be possible in which the conditions of the experiment are changed slightly to alter the ratio of the two components in the composite spectrum, in which case a linear combination of the composite spectra can be used to generate the two component spectra (Brotherus et al., 1980). The arbitrariness of many of these procedures has been demonstrated by McIntyre et al. (1982), who showed that the estimated fraction of immobilized lipid in a composite spectrum varied between 30% and 85%, depending on which spectrum was chosen as the first component in the subtraction procedure. Of course, if more than one pair of component spectra can be used to simulate the composite spectrum, with different proportions of the two components for the different pairs of spectra, then no definitive solution is possible. However, the range of possible solutions can be limited if it is

† The Science and Engineering Research Council is thanked for financial support.

‡ Department of Biochemistry.

§ Department of Physics.

[1] Abbreviations: ESR, electron spin resonance; DOPC, dioleoylphosphatidylcholine.

0006-2960/85/0424-2615$01.50/0

required that the nature of the component spectra (order parameters and line widths) and their amount should change smoothly with variables such as the lipid to protein ratio and the temperature. Because of the difficulty in choosing the "correct" components for subtraction, and because of the need to analyze a large number of spectra, we have developed a new computerized procedure for selection of the two components and for subtraction, based on a variational procedure.

It has been shown that simple decomposition of a composite ESR spectrum into two component spectra will be in error if the rate of exchange between the two environments is significant on the ESR time scale (Davoust & Devaux, 1982). In this region of exchange times, ESR spectra should be sensitive to the rate of exchange, and the rate should be obtainable from the spectra. We show here that, for the (Ca^{2+},Mg^{2+})-ATPase system, the rate of exchange probably is significant and thus that ESR can be used to estimate exchange times.

Materials and Methods

Lipids were obtained from Lipid Products, and spin-labeled stearic acid was prepared from 12-hydroxystearic acid (Fluka) by the method of Waggoner et al. (1969). Spin-labeled phosphatidylcholine was synthesized by condensing the spin-labeled fatty acid with lysophosphatidylcholine as outlined in Boss et al. (1975). It ran as a single spot on thin-layer chromatography with a retention time similar to that of dioleoylphosphatidylcholine.

The spin-labeled phospholipid was introduced into (Ca^{2+},Mg^{2+})-ATPase at various phospholipid to protein ratios by using a modification of the method outlined in East & Lee (1982). Briefly, sarcoplasmic reticulum (SR) was prepared from muscle as described (East & Lee, 1982). Spin-labeled phosphatidylcholine (0.15 mg) was dried to a thin film on 3-mL glass tubes, and 500 μL of the SR suspension (19 mg of protein mL^{-1}) was added. The sample was sonicated in a sonication bath for 20 s. Aliquots (40, 80, and 150 μL) of cholate (100 mg mL^{-1}) in phosphate buffer [potassium phosphate (50 mM), sucrose (250 mM), KCl (1.0 M), pH 8.0] were added to the SR with rapid stirring. The solubilized SR was loaded onto a sucrose gradient (3.5 mL of 30% sucrose plus a cushion of 60% and 80% sucrose) and centrifuged (300000g, 6 h). The ATPase formed a narrow band at the 30–60% interface and was removed with a Pasteur pipet, washed twice by further centrifugation in phosphate buffer, and resuspended in buffer at a protein concentration of around 5 mg mL^{-1}. As described previously, excess lipid and detergent remained at the top of the sucrose gradient (Warren et al., 1974). Samples were stored at −20 °C.

ATPase activity was measured as described in Rooney & Lee (1983) at 37 °C, pH 7.2, pCa^{2+} = 6.0, and ATP = 2 mM. Since the membrane samples prepared by the above procedures were in the form of sheets and unsealed vesicles, ATPase activity is fully uncoupled with no accumulation of Ca^{2+}. Protein was estimated by use of the extinction coefficient given by Hardwicke & Green (1974). Phospholipids were estimated by the method of Bartlett (1969) after extraction in chloroform, methanol, and water (Bligh & Dyer, 1959). The ATPase isolated at the three cholate concentrations given above contained 71, 28, and 17 lipids per protein with ATPase activities of 13, 12, and 8 IU, respectively. The ATPase activity at 17 lipids per protein varies somewhat between samples but is typically 50% of that at 30 lipids per protein.

ESR experiments were performed with a Bruker ER200D spectrometer in the absorption mode. Samples were contained in capillary tubes, and the temperature was controlled to within 0.5 °C with a Bruker B-ST 100/700 variable temperature controller. Spectra were recorded with phase-sensitive detection at 100 kHz, the peak-to-peak modulation amptitude being 2.5 G and the microwave power setting being 10 mW. Spectra were digitized, averaged, stored, and manipulated in a Z-80-based microcomputer system, 1000 data points being taken for a scan width of 100 G. Spectra were integrated by using the trapezoid method. All temperature effects were reversible: after cycling between 0 and 37 °C, identical spectra could be obtained on a second temperature cycle. Samples were not degassed.

Under the conditions used for the ESR experiments, a significant background signal was obtained from the glass capillaries and quartz cooling system. A standard background spectrum was therefore automatically subtracted from all spectra by using an iterative process based on the requirement that the first integral should begin and end at zero with no significant negative values. After background subtraction, all spectra were scaled to equal second integrals. For spectral subtraction it was important to ensure that the horizontal alignments of the spectra were consistent. Spectra were aligned on the basis of the point at which the high-field side of the central peak crossed the base line. Spectral simulations (see below) showed that this point shifted by ca. 0.8 G with changing order parameters from 0.90 to 0.05 and thus that the crossover point for the immobilized and mobile spectra used in spectral subtractions (see below) differed by 0.6 G. This difference was incorporated into the alignment procedure but had an insignificant effect on the results for the relatively broad spectra obtained here. ESR spectra were simulated by using the method of Israelachvili et al. (1976), assuming that the spin-labeled lipid undergoes complete axial rotation about its long molecular axes while it tumbles rapidly within the confines of a cone. Residual line widths were assumed to be of the form $b + c\cos^2\beta$ as suggested by Schindler & Seelig (1973) rather than of the mixed Lorentzian–Gaussian form used by Israelachvili et al. (1976).

The composite ESR spectra obtained for the (Ca^{2+},-Mg^{2+})-ATPase system were fitted to the sum of two component spectra as follows. The intensity of the composite spectrum I_c at any given field position can be written as

$$I_c = f_1 I_1 + f_2 I_2 \quad (1)$$

$$I_c = f_1 I_1 + (1 - f_1) I_2 \quad (2)$$

where f_1 and f_2 are the fractions of components 1 and 2 in the composite spectrum and I_1 and I_2 are the intensities of the component spectra at the given field position, the composite spectrum and the two component spectra having been normalized to equal areas. Thus

$$0 = I_c - f_1 I_1 - (1 - f_1) I_2 \quad (3)$$

Our fitting procedure is to calculate the difference D at any given field position for various values of the fraction f of component 1:

$$D = I_c - f I_1 - (1 - f) I_2 \quad (4)$$

If the component spectra have been chosen correctly, then the difference D will, in the absence of noise, be zero when $f = f_1$, the fraction of component 1 actually present in the composite spectrum. As f is varied from 0 to 1, the difference D will vary from negative to positive, passing through 0. Carrying out this calculation across the spectrum generates a set of difference spectra, as shown in Figure 1. The absolute values of D (that is, ignoring the sign of D) are then summed across the difference spectrum, and the fraction f giving the smallest sum is taken to be f_1. To allow comparison between

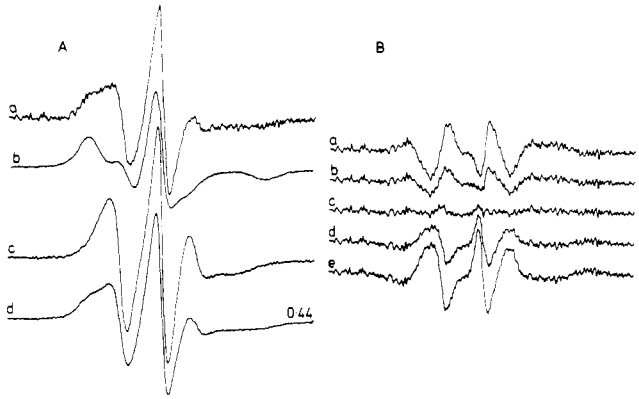

FIGURE 1: Determination of the mole fraction of immobile and mobile components in experimental spectra. Panel A: (a) ESR spectrum of lipid-depleted ATPase (17 lipids/protein), 29 °C; (b) immobile component, DOPC + cholesterol (1:1), −7 °C; (c) mobile component, DOPC, 17 °C; (d) composite spectrum, i.e., spectrum b + spectrum c (in ratio 0.44:0.56). Panel B: Residual spectra after subtracting composites of various mole fractions of the mobile and immobile components from the lipid-depleted ATPase spectrum (see Materials and Methods for details). The mole fraction for the immobile component is (a) 0.00, (b) 0.25, (c) 0.44, (d) 0.75, or (e) 1.00.

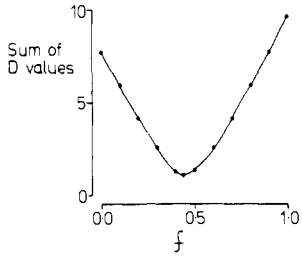

FIGURE 2: Variation of D_t values with fraction f of the immobile component for the system shown in Figure 1. The noise level subtracted from the sum of D values was 1.7.

spectra, an estimate of the noise level is subtracted from the sum of D values. This estimate is made by summing D values for the difference spectra over the first 50 data points, where simulations show no signal intensity, and extrapolating to 1000 points. Figure 2 illustrates the observed variation in the sum of D values calculated in this way (D_t), as a function of f. Because the component spectra used in the subtraction procedure have higher signal-to-noise ratios than the experimental composite spectrum, the noise level of the subtractions is dominated by that of the experimental composite spectrum and is thus independent of f.

The two component spectra required in the subtraction procedure were chosen from a set of spectra for the spin-labeled phospholipid in bilayers of dioleoylphosphatidylcholine and mixtures of dioleoylphosphatidylcholine and cholesterol at a 1:1 molar ratio, recorded at 4-deg intervals between 258 and 310 K. The choice of these two systems to generate the necessary library of component spectra was arbitrary but was found to cover the range of order parameters and correlation times necessary to fit the experimental composite spectra. We found no discontinuities in the ESR spectra on taking samples below the aqueous freezing point, as expected for probes that are sensitive only to motion in the bilayer phase. Spectra for spin-labeled phospholipid in bilayers of dipalmitoylphosphatidylcholine in the gel phase were found to exhibit very broad line widths, possibly caused by spin–spin exchange in clusters enriched in spin-labeled phospholipids: such spectra could not therefore be used in the fitting procedure. Our procedure for selecting the appropriate component spectra was as follows. First, an immobile component for the composite

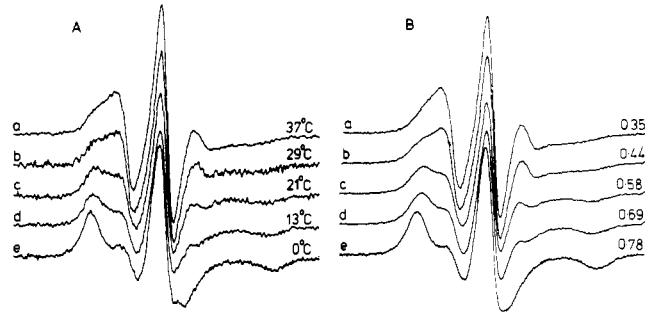

FIGURE 3: Panel A: ESR spectra of lipid-depleted ATPase (17 lipids/protein) at temperatures shown in the diagram. Panel B: Composite spectra, constructed from a mobile component (DOPC) and an immobile component [DOPC + cholesterol (1:1)], giving the best fit to the spectra in panel A. The mole fraction of the immobile component is shown in the diagram. Order parameters for the immobile component and correlation times for the mobile component are given in Figure 5.

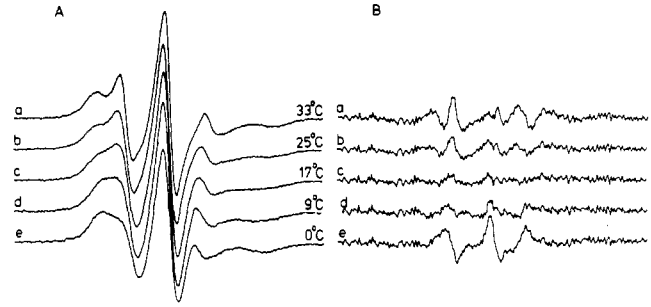

FIGURE 4: Determination of optimal mobile component. Panel A: Composite spectra constructed from the same immobile component [cholesterol + DOPC (1:1), −7 °C] and various mobile components (DOPC, temperatures given in diagram) giving the best fit to lipid-depleted ATPase (17 lipids/protein) at 29 °C. Panel B: Residual spectra after subtracting composite spectra shown in panel A from lipid-depleted ATPase spectrum (spectrum a in Figure 1A).

spectrum at the lowest lipid to protein ratio (Figure 3) was chosen by matching the observed maximum splittings. With this component fixed, the second, mobile component was chosen as that which gave the smallest D_t (as in Figure 4). The choice of the immobile component was then checked by fixing the mobile component and varying the immobile: the choice made by matching the maximum splitting was generally found to be the one giving the minimum D_t. Finally, the calculated composite spectrum is compared to the experimental spectrum to ensure that all features of the spectrum are reproduced faithfully. The procedure works well at low temperatures in that one particular pair of mobile and immobile components gives a lower value for D_t than any other pair, allowing an accurate determination of the fractions of the two components in the two-component model. At higher temperatures, however, it is found that a range of pairs of mobile and immobile components gives similar D_t values, although at different fractions of mobile and immobile components for each particular pair. It is thus not possible to obtain these fractions by using best fit to the experimental spectrum as the sole criterion of selection. In such cases we therefore introduce two further criteria. First, we compare the experimental and simulated spectra and choose only those that have the correct shape in the low- and high-field regions: the central peak makes a relatively large contribution to D_t when the peak is sharp, and small differences in peak width and peak position then become important. Second, we require that the mobile and immobile components should change smoothly with temperature and with composition. In practice we find that the main advantage of the difference method introduced here is

Table I: Selection of Component Spectra To Fit the Spectrum for the 17:1 Phospholipid:ATPase System at 29 °C

fixed component	variable component	min D_t	value of f_1 giving min D_t
DOPC/cholesterol, −7 °C	DOPC, 0 °C	3.8	0
	DOPC, 5 °C	1.7	0.07
	DOPC, 9 °C	1.3	0.28
	DOPC, 13 °C	1.3	0.37
	DOPC, 17 °C	1.0	0.44
	DOPC, 21 °C	1.4	0.49
	DOPC, 25 °C	2.1	0.54
	DOPC, 29 °C	2.9	0.64
DOPC, 17 °C	DOPC/cholesterol, −15 °C	1.4	0.40
	DOPC/cholesterol, −11 °C	1.1	0.42
	DOPC/cholesterol, −7 °C	1.0	0.44
	DOPC/cholesterol, −3 °C	1.1	0.47
	DOPC/cholesterol, 0 °C	1.5	0.44
	DOPC/cholesterol, 5 °C	1.2	0.51
	DOPC/cholesterol, 9 °C	1.4	0.55
	DOPC/cholesterol, 13 °C	2.6	0.65

that it allows the rapid scanning of a library of spectra for all possible pairs of spectra and so allows the use of a larger base set of component spectra than would be possible in a nonautomatic, manual procedure, with more subjective end-point criteria. Effective order parameters were calculated by using the equations of Gaffney (1976) for order parameters less than ca. 0.80 or were obtained by spectral simulation for larger values, and effective correlation times were estimated as in Likhtenshtein (1976).

Results

ESR spectra of phosphatidylcholine containing a C12-nitroxide-labeled stearic acid incorporated into the (Ca^{2+},-Mg^{2+})-ATPase system are clearly composed of more than one component. Such spectra are commonly fitted to sums of two components, a mobile component representing spin-labeled phospholipid in the bulk lipid phase and an immobile component representing spin-labeled phospholipid in the protein annulus. To quantitate the fractions of mobile and immobile component, it is necessary to be able to describe the line shapes of the two components. For the mobile component it is logical to choose from a set of spectra obtained from simple lipid bilayers over a range of temperatures, and this is the procedure commonly adopted (Jost & Griffith, 1978b). The choice of possible spectra for the immobile component is less obvious. The spectrum obtained at a low molar ratio of lipid to protein has sometimes been assumed to represent solely the immobilized component [see Jost & Griffith (1978b)], but this is inappropriate here as it does not, as demonstrated later. Silvius et al. (1984) have represented the immobile component by the spectrum in a 4:1 mixture of dipalmitoylphosphatidylcholine and palmitoyloleoylphosphatidylcholine at low temperature, and Ellena et al. (1983) have represented it by the spectrum in a mixture of ether, pentane, and ethanol at low temperature. We find that good fits to the experimental data can be obtained by selection of the immobile component from a set of spectra in a 1:1 molar ratio of dioleoylphosphatidylcholine and cholesterol: the relatively rigid cholesterol molecule is known to immobilize lipid fatty acyl chains in a manner that might be comparable to a protein surface.

According to the criterion of minimum D_t, these libraries of spectra are scanned to obtain pairs of spectra that best fit the experimental spectrum. The method is illustrated for the spectrum at a 17:1 lipid:ATPase molar ratio at 29 °C in Figures 1, 2, and 4 and Table I. The immobile component is first chosen by matching the splittings of the composite spectrum to one of the library of component spectra: in this case the best match is to the DOPC/cholesterol system at −7 °C. With this as the immobile component, the best possible fit (minimum D_t value) is then obtained with all the other library spectra to obtain the mobile component as that giving the lowest D_t value. The procedure is illustrated in Figure 4 and Table I, where it is clear that the best fit is obtained with DOPC at 17 °C as the mobile component. With the mobile component fixed, the immobile component can then be varied to show that the spectrum chosen by matching the observed splittings was indeed correct (Table I). The procedure is repeated with other component spectra to confirm that the chosen pair indeed produce the minimum D_t value. The sensitivity of the fit for any two component spectra to the assumed fraction of mobile and immobile components is illustrated in Figures 1 and 2.

At 0 °C the composite spectrum at a 17:1 lipid:ATPase molar ratio is dominated by the immobile component, so that this component is well-defined. The observed splittings match those for a 1:1 mixture of DOPC/cholesterol at −15 °C: maximum splittings for spectra in the DOPC/cholesterol system at −11 °C and higher temperatures are significantly too small to provide a good fit to the observed data. Since this spectrum is dominated by the immobile component, a relatively wide range of mobile components provides almost equally good fits. The lowest D_t value (1.2) is obtained with DOPC at 0 °C as the mobile component, but spectra up to ca. 17 °C (D_t = 1.8) provide reasonable fits. The mobile component is better defined at a 71:1 lipid:ATPase molar ratio. With the same immobile component as was used to fit the spectrum at a 17:1 lipid:ATPase molar ratio, the mobile component giving the best fit was still DOPC at 0 °C (D_t = 2.3), but now fits to other mobile components were significantly worse, that to DOPC at 5 °C, for example, giving a D_t value of 3.4. At the highest temperatures studied (37 °C) for the 17:1 lipid:ATPase molar ratio, equally good fits are obtained with the DOPC/cholesterol system at −7 to 0 °C as the immobile component (D_t = 1.2–1.4), with the mobile component represented by DOPC at 17 °C. Importantly, however, the calculated fraction of immobile component only varies between 0.34 and 0.37 over this range. Varying the mobile component to DOPC at either 13 or 21 °C gives significantly higher values for D_t (1.8 and 2.0) with calculated mole fractions of the immobile component of 0.28 and 0.40, respectively. If the immobile component for the 71:1 lipid:ATPase molar ratio is fixed as DOPC/cholesterol at 0 °C, then the mobile component is well-defined as DOPC at 29 °C (D_t = 1.5). Fits to DOPC at 25 and 33 °C give significantly worse fits with D_t values of 2.0 and 2.4, respectively. With the mobile component fixed as DOPC at 29 °C, the immobile component can be varied between DOPC/cholesterol at −7 and 9 °C (D_t values of 1.9 and 1.7, respectively), but with relatively little change in the mole fraction of immobile component (0.30–0.34).

Figure 5 illustrates the variation of the effective order parameter of the immobile component and the effective correlation time for the mobile component as a function of temperature and molar ratio of phospholipid to ATPase: the mobile component is too mobile to allow measurement of an order parameter. Variation of the fraction of the immobile component by more than 0.1 and of the other parameters by more than ±10% gives poor fits to the experimental data.

The calculated decrease in mole fraction of the immobile component with increasing temperature is too large to fit to any reasonable static two-component model (see Discussion). However, Davoust & Devaux (1982) have shown that such a decrease in immobile fraction can be artifactual if exchange

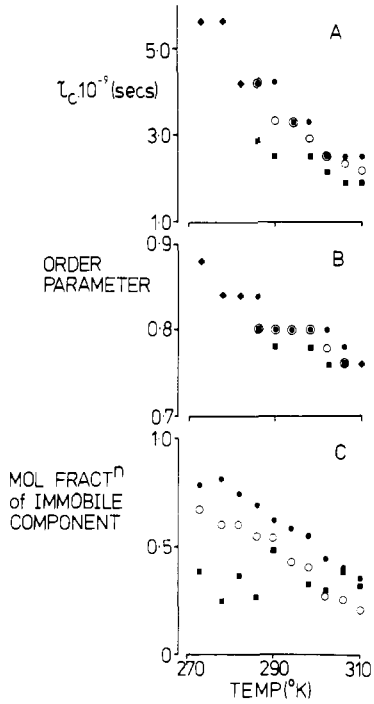

FIGURE 5: Summary of results obtained by using the best fit of mobile (DOPC) and immobile [DOPC + cholesterol (1:1)] components to the composite ATPase spectra. The correlation time (τ_c) for the mobile component, the effective order parameter for the immobile component, and the mole fraction of the immobile fraction giving the best fit by the spectral subtraction procedure are shown for high-lipid ATPase (71 lipids/protein) (■), intermediate-lipid ATPase (28 lipids/protein) (○), and lipid-depleted ATPase (17 lipids/protein) (●). The symbol ♦ is used where all three symbols overlap. Variation of the fraction of immobile component by more than 0.1 and of the other parameters by more than ±10% results in poor fits to the data.

occurs between environments at a rate comparable to the ESR time scale. They have presented the equations necessary to simulate ESR spectra showing exchange between bulk and annular lipid in two cases. The first assumes that the average orientation of the nitroxide label is preserved during the exchange and corresponds to a protein with a smooth surface. The second assumes that there is no correlation between the nitroxide orientation before and after exchange and corresponds to a protein with a rough surface. Spectra for the two components corresponding to bulk and annular phospholipid in the absence of exchange are calculated by assuming that the spectra can be represented by the sum of three Lorentzian lines with the positions of the low- ($m = +1$), central- ($m = 0$) and high-field ($m = -1$) lines being given by

$$H_m(\theta) = H_0 + \Delta H(\tfrac{2}{3} - \sin^2\theta) - m(T_\parallel'^2 \cos^2\theta + T_\perp'^2 \sin^2\theta)^{1/2}$$

where the term ΔH gives the shift due to the g-factor anisotropy, H_0 is the mean field position of the central line, $T_\parallel'$ and $T_\perp'$ are the principal values of the hyperfine splitting in the effective spin Hamiltonian $\mathcal{H}'$, and θ is the angle between the bilayer plane and the direction of the applied magnetic field (Devaux et al., 1973). As illustrated in Figure 6, we find that reasonable simulations can be obtained for the DOPC/cholesterol system and for the DOPC system at higher temperatures (>13 °C) for the low-field region of the spectrum, with less good agreement at high field. The parameters (in gauss) used in the simulations were as follows: for DOPC at 37 °C, line widths ($m = -1$, 0, +1) of 3.5, 3.0, and 5.0, $T_\parallel$ of 15.0, $T_\perp$ of 15.0, and ΔH of 1.0; for DOPC/cholesterol at −15 °C, line widths ($m = -1$, 0, +1) of 4.5, 4.0, and 5.0, $T_\parallel$

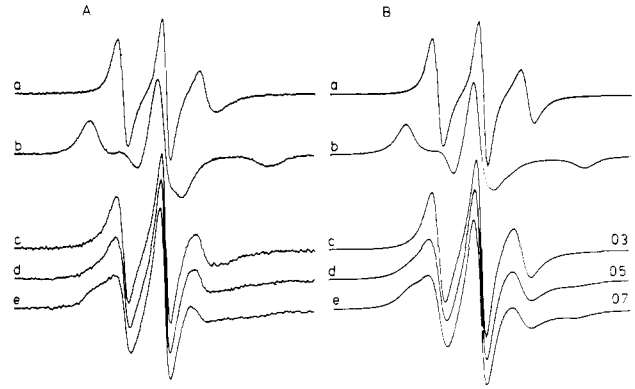

FIGURE 6: Panel A: ESR spectra of (a) DOPC, 37 °C (mobile component), (b) DOPC + cholesterol, −15 °C (immobile component), and (c–e) ATPase systems at lipid:protein ratios of (c) 71:1, (d) 28:1, and (e) 17:1, all at 37 °C. Panel B: Simulated spectra corresponding to spectra a–e, respectively, in panel A: (a, b) single-component spectra; (c–e) spectra calculated from the exchange model with an exchange time of 0.1 μs and a mole fraction of immobile component of (c) 0.3, (d) 0.5, or (e) 0.7.

of 30.0, $T_\perp$ of 8.0, and ΔH of 7.0. Line widths are defined as the maximum to minimum separation of the first derivative. For lower temperatures in the DOPC system, however, the simulations are poor. This problem with the simple simulations is well-known, and attempts to overcome it have been made by the introduction of anisotropic line widths [see Schindler & Seelig (1973) and Devaux et al. (1983)]. However, this is mathematically very complex for the exchange model. In fitting experimental spectra to the exchange model, we have therefore only considered the line shape of the low-field region: fortunately, spectra from the region of intermediate fluidity where the simulations are particularly poor are not relevant in our case. Figure 6 illustrates that it is possible to simulate spectra for the ATPase system by using the exchange model. We have used the second model of Davoust and Devaux for the simulations: this gives slightly better agreement than the first model although the difference is probably not significant. In all simulations we have taken the immobile component as that in DOPC/cholesterol mixtures at a molar ratio of 1:1 and at a temperature of −15 °C. For the mobile component we have taken the spectrum in DOPC at the temperature of the experiment. We find that it is possible to simulate the shape of the low-field peak in this way, although the overall splitting of the spectrum is too large, suggesting that the environmental polarities are different in the component and ATPase systems. Applying a simple polarity correction factor a/a' [see Gaffney (1976)] of 0.95 for the immobile component and 0.9 for the mobile component does not alter the shape of the spectrum but reduces the overall splitting to that observed experimentally (Figure 6). The mole fractions of the immobile component required to fit the experimental spectra at 37 °C are 0.7, 0.6, and 0.3 for lipid:ATPase molar ratios of 17:1, 28:1, and 71:1, respectively, with an exchange time τ_{BA} (time to jump from the bulk to the annular phase) of 0.1 μs. The average exchange rate ν_{ex} is defined by (Davoust & Devaux, 1982)

$$\nu_{ex} = f_A \tau_{AB}^{-1} = f_B \tau_{BA}^{-1}$$

where f_A and f_B are the fractions of lipid in the annular and bulk phases, respectively, and τ_{AB} and τ_{BA} are the probabilities per unit time for exchange between the annulus and the bulk and between the bulk and the annulus, respectively. As shown in Figure 7, good fits are also obtainable down to 13 °C, with slight increases in the mole fraction of the immobile component to 0.8, 0.7, and 0.45 for lipid:ATPase molar ratios of 17:1, 28:1, and 71:1, respectively, and zero exchange on the ESR time

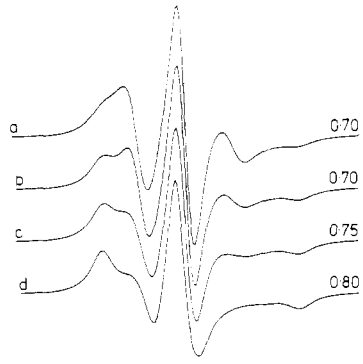

FIGURE 7: Simulations of ESR spectra of lipid-depleted ATPase (experimental spectra a–d shown in Figure 3A) at (a) 37, (b) 29, (c) 21, and (d) 13 °C, using simulated mobile and immobile components with exchange between the two environments (see Materials and Methods for details). The mole fraction of the immobile component is given in the diagram, and the exchange times are (a) 0.1, (b) 0.2, (c) 0.2, and (d) 0.5 μs.

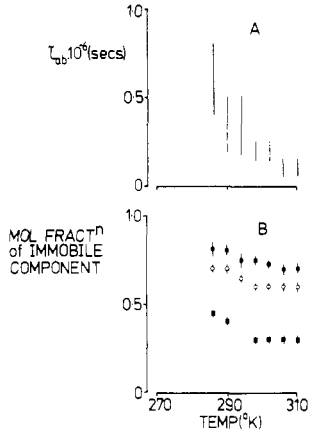

FIGURE 8: Summary of results obtained by using the best fit of simulated ESR spectra to ATPase spectra. The exchange time (τ_{AB}) between mobile and immobile environments and the mole fraction of immobile component required to give the best fit are shown for high-lipid ATPase (71 lipids/protein) (■), intermediate-lipid ATPase (28 lipids/protein) (○), and lipid-depeleted ATPase (17 lipids/protein) (●). Bars show the range of values for which acceptable fits were obtained.

scale (>1 μs). It was not possible to fit all the spectra at both high and low temperatures by using the same mole fractions for the immobilized component. Further, it was not possible to simulate the spectra by assuming a large (>0.1) decrease in order parameter for the immobile component with increasing temperature from 0 to 37 °C or by assuming no change in the mobile component with temperature. In the low-field region, experimental and simulated spectra are superimposable. Although, as already described, agreement is less good in the high-field region, the general changes in shape of the simulated spectra reproduce those found experimentally. Figure 8 illustrates the range of values for τ_{AB} and for f_A over which reasonable simulation of the experimental data could be achieved. No attempts were made to simulate spectra at temperatures below 13 °C because of the relatively poor simulations of the component spectra at these temperatures. As shown in Figure 8, there is a gradual increase in exchange time and increase in mole fraction of the immobile component with decreasing temperature over this range.

Discussion

ESR spectra of spin-labeled fatty acids and phospholipids incorporated into many membrane systems show the presence of (at least) two components, one immobilized and one relatively free (Jost & Griffith, 1978a,b). It has been suggested that the immobile component represents "trapped" lipid, immobilized between two or more proteins (Hoffmann et al., 1981; Andersen et al., 1981; Higashi & Kirino, 1983; Bittman, 1984). Andersen et al. (1981) studied the ATPase covalently modified with a spin-labeled fatty acid derivative and argued that the immobilized ESR signal could not be due to annular lipid, at least in part because of an increase in the proportion of immobilized lipid on cross-linking with glutaraldehyde. Thomas et al. (1982) however observed no change in the ESR spectrum for this same system when cross-linked with glutaraldehyde. Further, we have presented evidence for binding sites for fatty acids on the ATPase distinct from the lipid–protein interface (Simmonds et al., 1982; Lee et al., 1982) so that these probes cannot be assumed to be probing only the lipid component of the membrane. In our studies we have therefore used spin-labeled phospholipids. For two reasons we do not believe that the immobilized component that we observe is due to trapped lipid. First, the amount of such trapped lipid would be expected to decrease with increasing molar ratio of lipid to protein. This is not observed (Figure 5). Second, as shown in the Appendix, the extent of protein–protein interaction in these systems is expected to be very limited, at least for a random mixture of lipid and protein, so that random protein–protein contacts of the kind suggested by Hoffmann et al. (1981) will be rare and thus unlikely to trap much lipid. It seems most likely that the immobilized component represents phospholipids in contact with membrane proteins (annular phospholipids) and the mobile component the rest of the phospholipid making up the normal bilayer component of the membrane (Watts, 1981). Here we show that for the (Ca^{2+},Mg^{2+})-ATPase system purified from sarcoplasmic reticulum it is possible to use ESR spectra to estimate both the number of phospholipids binding to the ATPase in the membrane and the rate of exchange of phospholipids between the annular and bulk phospholipid phases. The first problem in estimating the numbers of phospholipids bound to the ATPase is in choosing the appropriate component spectra with which to fit the experimental composite spectrum. The importance of this problem has been demonstrated by McIntyre et al. (1981, 1982), who used four different subtraction procedures and obtained estimates of between 8 and 48 for the number of phospholipids immobilized on the ATPase at a total lipid:protein molar ratio of 60:1 at 4 °C. All four methods relied on subtraction of one assumed component from the composite spectrum until a spectrum was obtained that was judged suitable as a second component. To try to remove some of the subjectivity in the choice of end point in the subtraction procedure, we have introduced an alternative procedure employing a null end point that can be readily automated and that is relatively fast. The procedure allows both the selection of the two component spectra that best fit the composite spectrum and the estimation of their relative weights in the composite spectrum. The procedure works particularly well at lower temperatures (less than ca. 27 °C). At higher temperatures it is found that rather a large range of sets of composite spectra give equally good fits to the composite spectrum: as described below, this is probably at least in part because the fits obtained at higher temperatures are artifactual since they neglect exchange effects.

When the two-component procedure is used in the absence of exchange, the calculated fraction of immobile component decreases markedly with increasing temperature. If the immobile component does indeed represent annular phospholipid, then the decrease is more marked than can be accommodated

by any simple model. Aggregation of protein would lead to a decrease in the number of annular phospholipids, but simple calculations show that the total circumference of a protein aggregate is not very different from the sum of the circumferences of the component proteins, so that any change would, in fact, be relatively small. A more attractive hypothesis is, therefore, that the decrease in the calculated number of annular lipids is artifactual, due to exchange of phospholipids between the protein surface (annular phospholipids) and bulk phospholipid phases, which is fast on the ESR time scale. In this context fast exchange means that the exchange frequency V_{ex} is greater than $\gamma[T_{\parallel}(\text{annulus}) - T_{\parallel}(\text{bulk})]/2\pi$, where γ is the gyromagnetic ratio. We stress that both the static two-component model and the exchange model are capable of giving excellent fits to the experimental data and therefore that it is not possible to choose between the two models on the basis of the ESR results alone.

Davoust & Devaux (1982) have presented equations that allow the calculation of exchange-averaged ESR spectra for the case where the average orientation of the nitroxide is the same in the two environments and for the case of a rough protein surface where any orientation is possible on the protein surface. We find marginally better agreement with the latter model, although differences are slight. On the basis of the exchange model, it is possible to obtain reasonable simulations of the experimental data with only a slight decrease in the fraction of immobilized lipid with increasing temperature (Figure 8).

If the exchange model is correct, then at 37 °C the exchange time between annulus and bulk is ca. 10^{-7} s. In an NMR study of cytochrome *c* oxidase, Paddy et al. (1981) detected a lipid motion in the presence of protein that was not present in the absence of protein, with a correlation time of ca. 10^{-7} s, and suggested that this could represent exchange between annular and bulk lipid. The close agreement with our estimate of exchange rate is pleasing. The exchange time is about a factor of 2 less than the time for lipid exchange in the absence of protein. The diffusion coefficients for lipids in simple lipid bilayers have been estimated as ca. 2×10^{-8} cm^2 s^{-1} (Devaux & McConnell, 1972; Lee et al., 1973). The time to diffuse a lipid diameter of 5 Å is then 0.6×10^{-7} s.

It should be stressed that a relatively rapid exchange of lipid does not mean that, as has been claimed, there is only one homogeneous lipid environment in these systems [see, for example, Chapman (1983)]. There are two distinct lipid environments as far as the ATPase is concerned, and the environment actually sensed by the ATPase (the annular phospholipid) is less mobile than the bulk phospholipid phase. Interestingly, the order parameter of the immobile component appears to be relatively insensitive to temperature in that spectra over the temperature range 13–37 °C are fitted in the exchange model to the same immobile component. Previous studies have suggested a marked decrease in orde- for the immobile component with increasing temperature [see, for example, Davoust et al. (1980) and Watts et al. (1981)], but such an apparent decrease in order would be expected in the presence of exchange (see Figure 5).

If it is assumed that at a high molar ratio of lipid to protein (71:1) all of the annular sites of the ATPase are occupied by lipid, then the number of annular phospholipids would be 32 at low temperature and 22 at higher temperatures (from Figure 8). The reason for the apparent decrease at higher temperatures is unclear. These numbers can be compared to other estimates in the literature. Using a spin-labeled phospholipid, Nakamura & Ohnishi (1975) estimated that a total

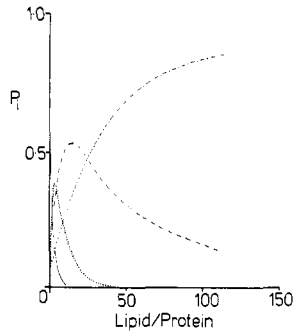

FIGURE 9: Variation of triangle probabilities with molar ratio of lipid to protein, assuming random mixing: (—) PPP, (···) PPL, (– –) PLL, and (–·–) LLL, where P and L represent protein and lipid, respectively.

of about 20 phospholipids could be immobilized by the ATPase at 22 °C, but this is probably an underestimate since in their subtraction procedure they assumed that the spectrum obtained at a 20:1 molar ratio of phospholipid to protein was all immobilized whereas our results (Figure 1) show that in fact such a spectrum contains a significant contribution from a mobile component. A number of studies using spin-labeled fatty acids have been interpreted in terms of between 20 and 24 annular sites (Jost & Griffith, 1978a; Thomas et al., 1982) although McIntyre et al. (1982) have estimated between 8 and 48. In a recent study, Silvius et al. (1984) using spin-labeled phospholipids have estimated 22 annular sites on the ATPase. Their analysis, however, was based on the assumption of effectively isolated ATPase molecules in the membrane, which will lead to some inaccuracy in the extrapolation procedure used (see Appendix).

X-ray scattering data for the ATPase were interpreted by Brady et al. (1982) in terms of a cylindrical structure for the ATPase, 142 Å high and 35.5 Å in diameter. The circumference of such a cylinder would be covered by 24 lipids in a bilayer arrangement if the surface area of a lipid molecule were typical of that in the liquid-crystalline phase (70 Å^2) and 32 lipids if the lipid surface area were typical of that in the gel phase (40 Å^2). These numbers agree well with the experiments described above and suggest that a decrease in the number of annular lipids with increasing temperature could follow from an increase in the apparent diameter of the lipid molecules with increasing temperature.

An important feature of the results presented above is that, at molar ratios of lipid to protein close to the number of annular lipid sites on the ATPase, both bulk and annular lipids are present, so that the ATPase molecules cannot have complete and independent annular shells. Rather, either phospholipids must be shared between the annuli of two or more proteins or there must be protein–protein contact. Unfortunately, it is not yet possible to calculate theoretically the number of annular lipids as a function of lipid to protein ratio: simple lattice models are inappropriate because of steric interactions between the very differently sized lipid and protein molecules. However, a simple model representing lipid and protein molecules as disks in the plane of the membrane can be used to estimate the number of lipid–lipid, lipid–protein, and protein–protein contacts for random mixing of lipids and proteins (see the Appendix). Interestingly, the model shows that for random mixing the probability of protein–protein contact is very low in the native membrane at a phospholipid:protein molar ratio of 90:1. Significant protein–protein contact would only occur below a phospholipid to protein ratio of ca. 20–30, at which point there must be many phospholipids shared between the annuli of two or more proteins. Since ATPase activity drops significantly at phospholipid to protein

ratios below ca. 30 (Warren et al., 1974), this suggests that random protein–protein contact could lead to loss of activity.

ACKNOWLEDGMENTS

We thank Dr. G. J. Daniell for suggesting the maximum entropy approach.

APPENDIX

Dodds (1975) has developed a simple statistical model of random disk packing applicable to mixtures of disks of two different sizes. He assumes that the randomly packed arrangement can be divided into a collection of triangles of only four distinct types. In the present problem, this corresponds to LLL, LLP, LPP, and PPP triangles, where L and P represent lipids and proteins, respectively. The model assumes therefore that each disk is in contact with its neighbors and is limited to a maximum P/L radius ratio of 6.46:1. The frequencies of each of the four triangle types are calculated for a given mixture of disks by a combinatorial method, and the resultant cubic equation is solved numerically.

An alternative approach to the calculation of triangle frequencies is based on the principle of maximizing entropy (Jaynes, 1958) subject to the physical constraints that exist in the system. This method is maximally noncommital with respect to unknown information and therefore produces the distribution corresponding to the minimum of initial assumptions.

In the present problem we maximize the entropy

$$S = -\sum_i p_i \ln p_i \qquad \text{(A-1)}$$

where p_i (i = 1–4) are the probabilities of the four allowed types of triangles, subject to two constraints:

$$\sum_i A_i p_i = A_{av} \qquad \text{(A-2)}$$

$$\sum_i N_i p_i = f_p \qquad \text{(A-3)}$$

where the A_i are the allowed triangle areas, A_{av} is the average triangle area in the membrane, N_i is the number of proteins in triangle of type i, and f_p is the mole fraction of protein in the membrane.

This maximization process leads simply to a relation of the Maxwell–Boltzmann form:

$$p_i = g_i \exp(\beta A_i + \gamma N_i)/Z \qquad \text{(A-4)}$$

where β and γ are Lagrange multipliers, g_i is the degeneracy of triangle type i (g_i = 1 for LLL and PPP and g_i = 3 for LLP and LPP), and Z is the partition function

$$Z = \sum_i g_i \exp(\beta A_i + \gamma N_i) \qquad \text{(A-5)}$$

To apply the constraint of eq A-3, we need a value of A_{av} for a particular mole fraction f_p. For close-packed structures of this type we can approximate A_{av} as being linearly related to f_p. That is

$$A_{av} = A_{LLL} + (A_{PPP} - A_{LLL})f_p \qquad \text{(A-6)}$$

where A_{LLL} and A_{PPP} are areas of LLL and PPP triangles, respectively.

This direct relationship between A_{av} and f_p makes the constraints of eq A-2 and A-3 equivalent. Thus, we can eliminate the Lagrange multiplier γ in eq A-4 and A-5, giving for the triangle probabilities

$$p_i = g_i \exp(\beta A_i)/Z \qquad \text{(A-7)}$$

$$Z = \sum_i g_i \exp(\beta A_i) \qquad \text{(A-8)}$$

The method of solution is to choose a range of β values (typically between −10 and +10) and for each one to solve eq A-8 and then eq A-7 to give a p_i for each triangle type. Substitution in eq A-2 and use of eq A-6 give the mole fractions corresponding to these probabilities. In the calculations we have assumed that the two halves of the bilayer are identical.

Figure 9 shows the calculated triangle probabilities as a function of lipid to protein ratio in the membrane assuming a ratio of protein to lipid radii of 4:1, corresponding to a maximum number of annular phospholipids around each protein of 32. It is clear that the probability of protein–protein contacts (given by the frequencies of LPP and PPP triangles) is low at lipid to protein molar ratios greater than ca. 20–30. This result follows from the much greater number of phospholipid molecules to protein molecules in the membrane, which makes the probability of lipid–protein contacts much higher than that of protein–protein contacts. Thus, for most of the mixtures studied here, extensive protein–protein contact is unlikely, and lipid trapped in protein clusters is an unlikely explanation for the observed immobilized component in the ESR spectra. The low probability of protein–protein contacts at lipid to protein molar ratios greater than ca. 20–30 also implies that lipid molecules must be shared between the annuli of two or more protein molecules. It cannot therefore be assumed that the extrapolation of plots of free phospholipid/bound phospholipid vs. molar ratio of phospholipid/protein to the point where free phospholipid/bound phospholipid is zero will necessarily give the number of annular sites [see Silvius et al. (1984)]. Such an extrapolation would be accurately true if random protein–protein contacts were highly unfavorable and if lipid molecules could not be shared between annuli—that is, if the protein molecules were effectively isolated in the membrane. The experimental results presented above suggest that this is unlikely.

Of course, the model analyzed here is highly simplified, but we stress that it makes the minimum number of initial assumptions and is therefore a suitable starting point for calculation. Thomas et al. (1982) detected much slower motion of the ATPase at a lipid:protein molar ratio of 37:1 than at 90:1, which could be due to protein–protein interaction. Since the random mixing model shows little protein–protein contact at this point, this could suggest that protein–protein contact is favorable energetically. It has recently been shown that ATPase dimers will aggregate into extensive "ladder"-like structures in the presence of vanadate (Dux & Martonosi, 1983; Buhle et al., 1983), and it is possible that structures of this type could form at low molar ratios of lipid to protein. Another possibility is that the hydrophilic portion of the ATPase has a greater cross-sectional area than the hydrophobic part [see La Maire et al. (1981)] so that the former will come into contact, causing protein immobilization before there is significant contact between the hydrophobic portions of the protein.

Registry No. ATPase, 9000-83-3; DOPC, 10015-85-7.

REFERENCES

Andersen, J. P., Fellmann, P., Moller, J. V., & Devaux, P. F. (1981) *Biochemistry 20*, 4928–4936.

Bartlett, G. R. (1959) *J. Biol. Chem. 234*, 466–468.

Bittman, R., Sakaki, T., Tsuji, A., Devaux, P. F., & Ohnishi, S. I. (1984) *Biochim. Biophys. Acta 769*, 85–95.

Bligh, E. G., & Dyer, W. J. (1959) *Can. J. Biochem. Physiol. 37*, 911–917.

Boss, W. F., Kelley, C. J., & Landsberger, F. R. (1975) *Anal. Biochem. 64*, 289–292.

Brady, G. W., Fein, D. B., Harder, M. E., & Meissner, G. (1982) *Biophys. J. 37*, 637–645.

Brotherus, J. R., Jost, P. C., Griffith, O. H., Keana, J. F. W., & Hokin, L. E. (1980) *Proc. Natl. Acad. Sci. U.S.A. 77*, 272–276.

Buhle, E. L., Knox, B. E., Serpersu, E., & Aebi, U (1983) *J. Ultrastruct. Res. 85*, 186–203.

Chapman, D. (1983) *Membr. Fluid. Biol. 2*, 5–42.

Davoust, J., & Devaux, P. F. (1982) *J. Magn. Reson. 48*, 475–494.

Davoust, J., Bienvenue, A., Fellmann, P., & Devaux, P. F. (1980) *Biochim. Biophys. Acta 596*, 28–42.

Devaux, P., & McConnell, H. M. (1972) *J. Am. Chem. Soc. 94*, 4475–4480.

Devaux, P., Scandella, C. J., & McConnell, H. M. (1973) *J. Magn. Reson. 9*, 474–485.

Dodds, J. A. (1975) *Nature (London) 256*, 187–189.

Dux, L., & Martonosi, A. (1983) *J. Biol. Chem. 258*, 2599–2603.

East, J. M., & Lee, A. G. (1982) *Biochemistry 21*, 4144–4151.

Ellena, J. F., Blazing, M. A., & McNamee, M. G. (1983) *Biochemistry 22*, 5523–5535.

Gaffney, B. J. (1976) in *Spin Labeling* (Berliner, L. J., Ed.) pp 567–571, Academic Press, New York.

Griffith, O. H., Baumeister, J. G., & Jost, P. C. (1982) *Biophys. J. 37*, 152–154.

Hardwicke, P. M. D., & Green, N. M. (1974) *Eur. J. Biochem. 42*, 183–193.

Higashi, K., & Kirino, Y. (1983) *J. Biochem. (Tokyo) 94*, 1769–1779.

Hoffmann, W., Pink, D. A., Restall, J., & Chapman, D. (1981) *Eur. J. Biochem. 114*, 585–589.

Israelachvili, J., Sjosten, J., Eriksson, L. E. G., Ehrstrom, M., Graslund, A., & Ehrenberg, A. (1976) *Biochim. Biophys. Acta 382*, 125–141.

Jaynes, E. T. (1958) *Probability Theory in Science and Engineering: Colloquium Lectures in Pure and Applied Science*, No. 4, Socony Mobil Oil Co., Dallas, TX.

Jost, P. C., & Griffith, O. H. (1978a) in *Biomolecular Structure and Function* (Agrio, P. F., Ed.) pp 25–54, Academic Press, New York.

Jost, P. C., & Griffith, O. H. (1978b) *Methods Enzymol. 49*, 369–418.

Lee, A. G., Birdsall, N. J. M., & Metcalfe, J. C. (1973) *Biochemistry 12*, 1650–1659.

Lee, A. G., East, J. M., Jones, O. T., McWhirter, J., Rooney, E. K., & Simmonds, A. C. (1982) *Biochemistry 21*, 6441–6446.

Le Maire, M., Moller, J. V., & Tardieu, A. (1981) *J. Mol. Biol. 150*, 273–296.

Likhtenshtein, G. I. (1976) *Spin Labeling Methods in Molecular Biology*, Wiley, New York.

London, E., & Feigenson, G. W. (1981) *Biochemistry 20*, 1939–1948.

McIntyre, J. O., Samson, P., Dalton, L. A., & Fleischer, S. (1981) *Biophys. J. 33*, 86a.

McIntyre, J. O., Samson, P., Brenner, S. C., Dalton, L., Dalton, L., & Fleischer, S. (1982) *Biophys. J. 37*, 53–56.

Nakamura, M., & Ohnishi, S. (1975) *J. Biochem. (Tokyo) 78*, 1039–1043.

Paddy, M. R., Dahlquist, F. W., Davis, J. H., & Bloom, M. (1981) *Biochemistry 20*, 3152–3162.

Rooney, E. K., & Lee, A. G. (1983) *Biochim. Biophys. Acta 732*, 428–440.

Schindler, H., & Seelig, J. (1973) *J. Chem. Phys. 59*, 1841–1850.

Silvius, J. R., McMillen, D. A., Saley, N. D., Jost, P. C., & Griffith, O. H. (1984) *Biochemistry 23*, 538–547.

Simmonds, A. C., East, J. M., Jones, O. T., Rooney, E. K., McWhirter, J., & Lee, A. G. (1982) *Biochim. Biophys. Acta 693*, 398–406.

Thomas, D. D., Bigelow, D. J., Squier, T. C., & Hidalgo, C. (1982) *Biophys. J. 37*, 217–222.

Waggoner, A. S., Kingzett, T. J., Rottschaefer, S., & Griffith, O. H. (1969) *Chem. Phys. Lipids 3*, 245–253.

Warren, G. B., Toon, P. A., Birdsall, N. J. M., Lee, A. G., & Metcalfe, J. C. (1974) *Biochemistry 13*, 5501–5507.

Watts, A. (1981) *Nature (London) 294*, 512–513.

Watts, A., Volotovski, I. D., & Marsh, D. (1979) *Biochemistry 18*, 5006–5013.

Watts, A., Davoust, J., Marsh, D., & Devaux, P. F. (1981) *Biochim. Biophys. Acta 643*, 673–676.